

## Homochiral Column Structure of *rac*- and $\Lambda$ -Tris(ethylenediamine)cobalt(III) Cyclotriphosphate Dihydrate in Crystal Structures and Cation–Anion Association in Aqueous Solution

Toshio Nakashima,<sup>\*,†</sup> Junichi Mishiro,<sup>†</sup> Masami Ito,<sup>‡</sup> Genichiro Kura,<sup>§</sup> Yuichi Ikuta,<sup>||</sup> Naohide Matsumoto,<sup>||</sup> Kiyohiko Nakajima,<sup>⊥</sup> and Masaaki Kojima<sup>#</sup>

Department of Chemistry, Faculty of Education and Welfare Science, Oita University, Dan-noharu, Oita 870-1192, Japan, Department of Chemistry, Fukuoka University of Education, Akama, Munakata, Fukuoka 811-4192, Japan, Department of Chemistry, Faculty of Science, Kumamoto University, Kurokami, Kumamoto 860-8555, Japan, Department of Chemistry, Aichi University of Education, Igaya, Kariya 448-8542, Japan, and Department of Chemistry, Faculty of Science, Okayama University, Tsushima-naka, Okayama 700-8530, Japan

Received September 27, 2002

*rac*- and  $\Lambda$ -tris(ethylenediamine)cobalt(III) cyclotriphosphate dihydrate with the chemical formulas *rac*-[Co(en)<sub>3</sub>]-P<sub>3</sub>O<sub>9</sub>·2H<sub>2</sub>O (**1**) and  $\Lambda$ -[Co(en)<sub>3</sub>]-P<sub>3</sub>O<sub>9</sub>·2H<sub>2</sub>O (**2**) were synthesized, and their crystal structures were determined by single-crystal X-ray analyses. In **1**, the cationic complex molecule [Co(en)<sub>3</sub>]<sup>3+</sup> with the  $\Delta$  or  $\Lambda$  enantiomer and cyclotriphosphate anion are alternately arrayed and connected by multiple hydrogen bonds to form a homochiral column structure. Adjacent homochiral columns with different chirality for **1** are connected by intercolumn hydrogen bonds through P<sub>3</sub>O<sub>9</sub><sup>3-</sup> anions, as the bridging groups, to form a tetrameric cyclic cylindrical structure, while the adjacent columns with the same chirality are connected for **2** to form the cyclic cylindrical structure. All 6 amino groups per [Co(en)<sub>3</sub>]<sup>3+</sup> participate in the formation of 12 hydrogen bonds, in which 8 hydrogen bonds contribute to the construction of a homochiral column and the remaining 4 hydrogen bonds contribute to the intercolumn interactions. The circular dichroism spectrum of the aqueous solution of  $\Lambda$ -[Co(en)<sub>3</sub>]<sup>3+</sup> changes drastically when excess P<sub>3</sub>O<sub>9</sub><sup>3-</sup> is added, and this change is explained by ion-pair formation. The thermodynamic association constant of [Co(en)<sub>3</sub>]<sup>3+</sup> with P<sub>3</sub>O<sub>9</sub><sup>3-</sup>, calculated from the conductivity data, was log *K* = 4.26 at 25 °C.

### Introduction

Since the historic discovery of spontaneous resolution by Louis Pasteur,<sup>1</sup> chirality has been an important topic in chemistry, pharmacy, and living organisms.<sup>2–4</sup> Chirality has also been a subject of continuous interest in coordination chemistry since Alfred Werner's time. Although Werner

published the first successful resolution of a metal complex in 1911,<sup>5</sup> he conjectured as early as 1899 that octahedrally coordinated metal complexes should occur in nonidentical mirror image isomers.<sup>6</sup> Presently, the interest in chirality in coordination compounds is booming, mainly because of the importance of optically active coordination compounds in enantioselective homogeneous catalysis.

When chiral molecules aggregate and crystallize, they can form one of the following: (1) a racemic compound; (2) a conglomerate (racemic mixture); (3) a racemic solid solution.<sup>7</sup> If enantioselective homochiral molecular discrimination arises from substantially strong, selective, and directional

\* To whom correspondence should be addressed. E-mail: nakashi@cc.oita-u.ac.jp. Fax: +81-97-554-7554.

† Faculty of Education and Welfare Science, Oita University.

‡ Research and Development Center, Oita University.

§ Fukuoka University of Education.

|| Kumamoto University.

⊥ Aichi University of Education.

# Okayama University.

(1) Pasteur, L. *Ann. Chim. Phys.* **1848**, *24*, 442–459.

(2) (a) Noyori, R. *Asymmetric Catalysis in Organic Synthesis*; John Wiley & Sons: New York, 1994. (b) Palyi, G.; Zucchi, C.; Caglioti, L. *Advances in Biochirality*; Elsevier: Oxford, U.K., 1999.

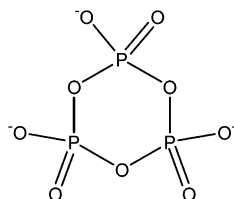
(3) (a) Prins, L. J.; Huskens, J.; Jong, F.; Timmerman, P.; Reinhoudt, D. N. *Nature* **1999**, *398*, 498–502. (b) Soo, J.; Whang, D.; Lee, H.; Jun, S. I.; Oh, J.; Jeon, Y. J.; Kim, K. *Nature* **2000**, *404*, 982–986.

(4) (a) Lehn, J.-M. *Supramolecular Chemistry, Concepts and Perspectives*; VCH: Weinheim, Germany, 1995. (b) Geib, S. J.; Vicent, C.; Fan, E.; Hamilton, A. D. *Angew. Chem., Int. Ed. Engl.* **1993**, *32*, 119–121. (c) Woods, C. R.; Benaglia, M.; Cozzi, F.; Siegel, J. S. *Angew. Chem., Int. Ed. Engl.* **1996**, *35*, 1830–1833.

(5) Werner, A. *Ber. Dtsch. Chem. Ges.* **1911**, *44*, 1887–1898.

(6) Werner, A. *Z. Anorg. Chem.* **1899**, *21*, 145.

Chart 1. Cyclo-3-phosphate



interactions, such as coordination bonds<sup>8</sup> or hydrogen bonds,<sup>9</sup> extending from two adjacent molecules to one-dimensional (1D), 2D, and 3D systems, then a conglomerate exhibiting 3D intermolecular homochiral interactions, and hence showing spontaneous resolution upon crystallization, would then be achieved. Although the recent extensive development of supramolecular chemistry and crystal engineering makes it possible to construct an assembly with specific network topologies, designing a conglomerate by these methods would be most difficult.

We have studied previously a cobalt(III) complex with a tripod ligand, [CoH<sub>3</sub>L]<sup>3+</sup> (H<sub>3</sub>L = tris[2-((imidazol-4-yl)methylidene)amino]ethylamine), and reported a process of self-assembly of achiral components to a chiral metal complex molecule, a homochiral 2D layer, and finally the conglomerate. During this process the formally hemi-deprotonated species [CoH<sub>1.5</sub>L]<sup>1.5+</sup> functions as a self-complementary chiral building block and generates equal numbers of protonated and deprotonated molecules to form an extended 2D homochiral layer structure due to the intermolecular hydrogen bonds.<sup>10</sup> The cation–anion ion-pair assembly process, in which either or both of the cations and anions is or are chiral species, is an alternative method for constructing an assembly network structure instead of the self-assembly process of a single self-complementary molecule. It has been known that ion-pair formation between a chiral cation [Co(en)<sub>3</sub>]<sup>3+</sup> and phosphates affects the CD spectrum.<sup>11</sup> In this study, the cation–anion assembly between [Co(en)<sub>3</sub>]<sup>3+</sup> and cyclotriphosphate, P<sub>3</sub>O<sub>9</sub><sup>3-</sup>, as a new phosphate has been examined (Chart 1). We have found that the cationic complex

- (7) (a) Eliel, E. L. *Stereochemistry of Carbon Compounds*; McGraw-Hill: New York, 1962. (b) Collet, A.; Brienne M–J.; Jacques, J. *Chem. Rev.* **1980**, *80*, 215–230. (c) Jacques, J.; Collet, A.; Wilen, S. H. *Enantiomers, Racemates and Resolutions*; John Wiley & Sons: New York, 1981. Jacques, J.; Leclercq, M.; Brienne, M.-J. *Tetrahedron* **1981**, *37*, 1727–1733. (d) Brock, C. P.; Schweizer, W. B.; Dunitz, J. D. *J. Am. Chem. Soc.* **1991**, *113*, 9811–9820. (e) Kuroda, R.; Mason, S. F. *J. Chem. Soc., Dalton Trans.* **1981**, 1268–1273. (b) Brock, C. P.; Dunitz, J. D. *Chem. Mater.* **1994**, *6*, 1118–1127.
- (8) (a) Hernandez-Molina, M.; Lloret, F.; Ruiz-Perez, C.; Julve, M. *Inorg. Chem.* **1998**, *37*, 4131–4135. (b) Lambert, F.; Renault, J.-P.; Policar, C.; M-Badaran, I.; Cesario, M. *Chem. Commun.* **2000**, 35–36. (c) Konno, T.; Chikamoto, Y.; Okamoto, K.; Yamaguchi, T.; Ito, T.; Hirotsu, M. *Angew. Chem., Int. Ed.* **2000**, *39*, 4098–4101.
- (9) (a) Seto, C. T.; Whitesides, G. M. *J. Am. Chem. Soc.* **1993**, *115*, 905–916. (b) Bishop, R. *Synlett* **1999**, 1351–1358. (c) Aoyama, Y.; Endo, K.; Anzai, T.; Yamaguchi, Y.; Sawaki, T.; Kobayashi, K.; Kanehisa, N.; Hashimoto, H.; Kai, Y.; Masuda, H. *J. Am. Chem. Soc.* **1996**, *118*, 5562–5571. (d) Tadokoro, M.; Isobe, K.; Uekusa, H.; Ohashi, Y.; Toyota, J.; Tashiro, K.; Nakasuji, K. *Angew. Chem., Int. Ed.* **1999**, *38*, 95–98. (e) Tadokoro, M.; Nakasuji, K. *Coord. Chem. Rev.* **2000**, *198*, 205–218.
- (10) (a) Katsuki, I.; Motoda, Y.; Sunatsuki, Y.; Matsumoto, N.; Nakashima, T.; Kojima, M. *J. Am. Chem. Soc.* **2002**, *124*, 629–640. (b) Shii, Y.; Motoda, Y.; Matsuo, T.; Kai, F.; Nakashima, T.; Tuchagues, J.-P.; Matsumoto, N. *Inorg. Chem.* **1999**, *38*, 3513–3522.
- (11) Duesler, E. N.; Raymond, K. N. *Inorg. Chem.* **1971**, *10*, 1486–1492.

Table 1. X-ray Crystallographic Data for *rac*-[Co(en)<sub>3</sub>]P<sub>3</sub>O<sub>9</sub>·2H<sub>2</sub>O (1) and  $\Lambda$ -[Co(en)<sub>3</sub>]P<sub>3</sub>O<sub>9</sub>·2H<sub>2</sub>O (2)

params	<i>rac</i> -[Co(en) <sub>3</sub> ]P <sub>3</sub> O <sub>9</sub> ·2H <sub>2</sub> O (1)	$\Lambda$ -[Co(en) <sub>3</sub> ]P <sub>3</sub> O <sub>9</sub> ·2H <sub>2</sub> O (2)
formula	C <sub>6</sub> H <sub>28</sub> N <sub>6</sub> O <sub>11</sub> P <sub>3</sub> Co	C <sub>6</sub> H <sub>28</sub> N <sub>6</sub> O <sub>11</sub> P <sub>3</sub> Co
fw	512.18	512.18
space group	<i>P</i> 2 <sub>1</sub> / <i>n</i> (No. 14)	<i>P</i> 2 <sub>1</sub> (No. 4)
<i>a</i> , Å	10.3442(7)	10.3594(8)
<i>b</i> , Å	13.5828(9)	13.5100(7)
<i>c</i> , Å	13.7851(8)	13.7923(8)
$\alpha$ , deg	90.00	90.00
$\beta$ , deg	94.815(2)	94.701(2)
$\gamma$ , deg	90.00	90.00
<i>V</i> , Å <sup>3</sup>	1930.0(2)	1923.8(2)
<i>Z</i>	4	4
<i>D</i> <sub>calc</sub> , g cm <sup>-3</sup>	1.763	1.768
$\mu$ , cm <sup>-1</sup>	12.03	12.06
<i>R</i> , <i>R</i> <sub>w</sub>	0.0581, 0.1648	0.0425, 0.1133

molecule with  $\Delta$  or  $\Lambda$  enantiomers is multiply hydrogen-bonded to the cyclotriphosphate anion to form a homochiral columnar structure. The crystal structures and the nature of the cation–anion interactions in aqueous solutions are reported.

## Results and Discussion

**Synthesis and Characterization.** Sodium cyclotriphosphate, Na<sub>3</sub>P<sub>3</sub>O<sub>9</sub>, was prepared by thermal condensation of NaH<sub>2</sub>PO<sub>4</sub>. Sodium cyclotriphosphate is known to exist in various states of hydration, Na<sub>3</sub>P<sub>3</sub>O<sub>9</sub>, Na<sub>3</sub>P<sub>3</sub>O<sub>9</sub>·H<sub>2</sub>O, Na<sub>3</sub>P<sub>3</sub>O<sub>9</sub>·3/2H<sub>2</sub>O, Na<sub>3</sub>P<sub>3</sub>O<sub>9</sub>·3H<sub>2</sub>O, and Na<sub>3</sub>P<sub>3</sub>O<sub>9</sub>·6H<sub>2</sub>O. Thermogravimetric (TG) analysis revealed that the compound that we prepared was the monohydrate. *rac*-Tris(ethylenediamine)-cobalt(III) cyclotriphosphate dihydrate, *rac*-[Co(en)<sub>3</sub>]P<sub>3</sub>O<sub>9</sub>·2H<sub>2</sub>O, was prepared by slow evaporation of an aqueous solution containing *rac*-[Co(en)<sub>3</sub>]Cl<sub>3</sub>·3H<sub>2</sub>O and Na<sub>3</sub>P<sub>3</sub>O<sub>9</sub>·H<sub>2</sub>O. The operation was conducted at room or lower temperature to avoid hydrolysis of the cyclotriphosphate ring. The C, H, and N microanalyses agreed with the formula *rac*-[Co(en)<sub>3</sub>]P<sub>3</sub>O<sub>9</sub>·2H<sub>2</sub>O. The optically active form could not be obtained by this procedure due to the higher solubility of the cyclotriphosphate complex. We prepared  $\Lambda$ -[Co(en)<sub>3</sub>]P<sub>3</sub>O<sub>9</sub>·2H<sub>2</sub>O via a metathesis reaction. An aqueous solution of  $\Lambda$ -[Co(en)<sub>3</sub>]Cl<sub>3</sub>·H<sub>2</sub>O was added to a slurry of Ag<sub>3</sub>P<sub>3</sub>O<sub>9</sub>·H<sub>2</sub>O in water in a stoichiometric ratio. After removal of AgCl by filtration, slow evaporation of the resulting solution yielded  $\Lambda$ -[Co(en)<sub>3</sub>]P<sub>3</sub>O<sub>9</sub>·2H<sub>2</sub>O. This formula was confirmed by the C, H, and N microanalyses.

**Structural Descriptions of *rac*-[Co(en)<sub>3</sub>]P<sub>3</sub>O<sub>9</sub>·2H<sub>2</sub>O (1) and  $\Lambda$ -[Co(en)<sub>3</sub>]P<sub>3</sub>O<sub>9</sub>·2H<sub>2</sub>O (2).** Their crystallographic data are summarized in Table 1. Two compounds, *rac*-[Co(en)<sub>3</sub>]P<sub>3</sub>O<sub>9</sub>·2H<sub>2</sub>O (1) and  $\Lambda$ -[Co(en)<sub>3</sub>]P<sub>3</sub>O<sub>9</sub>·2H<sub>2</sub>O (2), crystallized in the monoclinic crystal system with similar cell dimensions, while the space groups of 1 and 2 are *P*2<sub>1</sub>/*n* and *P*2<sub>1</sub>, respectively. Selected bond distances with their estimated standard deviations in parentheses are given in Table 2. The hydrogen-bond distances less than 3.3 Å are summarized in Table 3.

Figure 1 shows the ORTEP drawing of *rac*-[Co(en)<sub>3</sub>]P<sub>3</sub>O<sub>9</sub>·2H<sub>2</sub>O (1) with the selected atom numbering schemes. The Co<sup>III</sup> ion has octahedral coordination geometry with the N<sub>6</sub> donor atoms belonging to three ethylenediamines. The Co–N

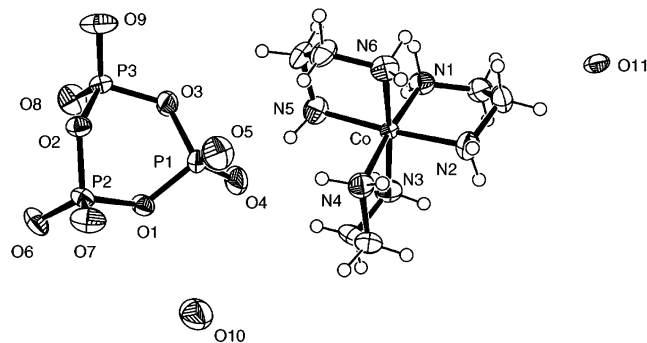
**Table 2.** Relevant Coordination Bond Distances (Å) for rac-[Co(en)<sub>3</sub>]P<sub>3</sub>O<sub>9</sub>·2H<sub>2</sub>O (1) and  $\Lambda$ -[Co(en)<sub>3</sub>]P<sub>3</sub>O<sub>9</sub>·2H<sub>2</sub>O (2)

rac-[Co(en) <sub>3</sub> ]P <sub>3</sub> O <sub>9</sub> ·2H <sub>2</sub> O (1)		$\Lambda$ -[Co(en) <sub>3</sub> ]P <sub>3</sub> O <sub>9</sub> ·2H <sub>2</sub> O (2)	
Co–N1	1.979(4)	Co–N1	1.966(4), 1.964(4)
Co–N2	1.973(4)	Co–N2	1.955(4), 1.972(4)
Co–N3	1.961(4)	Co–N3	1.968(4), 1.966(4)
Co–N4	1.968(4)	Co–N4	1.964(4), 1.953(4)
Co–N5	1.935(4)	Co–N5	1.970(4), 1.967(4)
Co–N6	1.962(4)	Co–N6	1.958(4), 1.956(4)

**Table 3.** Hydrogen-Bond Distances (Å) for rac-[Co(en)<sub>3</sub>]P<sub>3</sub>O<sub>9</sub>·2H<sub>2</sub>O (1) and  $\Lambda$ -[Co(en)<sub>3</sub>]P<sub>3</sub>O<sub>9</sub>·2H<sub>2</sub>O (2)<sup>a</sup>

rac-[Co(en) <sub>3</sub> ]P <sub>3</sub> O <sub>9</sub> ·2H <sub>2</sub> O (1)		$\Lambda$ -[Co(en) <sub>3</sub> ]P <sub>3</sub> O <sub>9</sub> ·2H <sub>2</sub> O (2)			
N1–O5 <sup>a</sup>	2.936(6)	N1–O15 <sup>b</sup>	3.202(6)	N7–O5 <sup>c</sup>	2.926(6)
N1–O9	2.926(5)	N1–O16	2.996(6)	N7–O21	2.909(6)
N2–O8 <sup>a</sup>	2.900(6)	N2–O18 <sup>b</sup>	2.707(6)	N8–O4	2.892(5)
N2–O11	2.981(6)	N2–O22	3.016(6)	N8–O6 <sup>c</sup>	2.913(5)
N3–O5 <sup>a</sup>	2.896(6)	N3–O15 <sup>b</sup>	2.795(6)	N9–O4	2.901(6)
N3–O11	2.854(6)	N3–O22	2.990(6)	N9–O9 <sup>c</sup>	2.885(5)
N4–O4	2.999(5)	N4–O7	2.869(6)	N10–O8 <sup>c</sup>	2.819(5)
N4–O8 <sup>a</sup>	2.902(5)	N4–O14 <sup>b</sup>	3.013(6)	N10–O17	2.915(5)
N5–O4	2.906(6)	N5–O7	3.019(6)	N11–O5 <sup>c</sup>	2.886(5)
N5–O7 <sup>a</sup>	2.800(5)	N5–O15 <sup>b</sup>	3.082(6)	N11–O17	3.268(6)
N6–O6 <sup>a</sup>	2.861(5)	N6–O14 <sup>b</sup>	3.072(6)	N12–O6 <sup>c</sup>	2.873(5)
N6–O9	2.903(5)	N6–O16	2.824(6)	N12–O21	2.875(6)
O10–O4	2.896(6)	O19–O15	3.026(8)	O21–O8	2.683(6)
O10–O8	3.020(7)	O19–O17	2.889(8)	O21–O13	2.682(6)
O11–O6	2.713(4)	O20–O5	2.985(8)	O22–O9	2.742(5)
O11–O7	2.728(4)	O20–O7	2.941(7)	O22–O14	2.795(6)

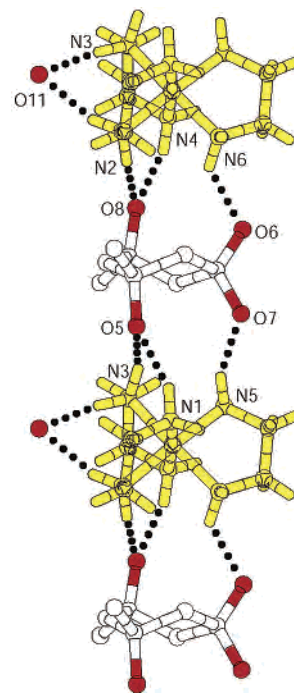
<sup>a</sup> a–c indicate contribution to the formation of the intracolumn hydrogen bonds.

**Figure 1.** ORTEP diagram of rac-[Co(en)<sub>3</sub>](P<sub>3</sub>O<sub>9</sub>)·2H<sub>2</sub>O (1) with displacement ellipsoids drawn at the 50% probability level and the selected atom labeling scheme.

distances are in the range reported for Co<sup>III</sup> complexes involving ethylenediamine.<sup>12</sup> The cationic complex [Co(en)<sub>3</sub>]<sup>3+</sup> assumes either a  $\Delta$  or  $\Lambda$  configuration, and two enantiomers are included in the crystal lattice. The anion P<sub>3</sub>O<sub>9</sub><sup>3-</sup> assumes a boat configuration, while the anions P<sub>3</sub>O<sub>9</sub><sup>3-</sup> in the other compounds reported so far usually assume a flat or chair conformation.<sup>13</sup> Day et al. reported that the flat or chair conformation of P<sub>3</sub>O<sub>9</sub><sup>3-</sup> is the preferable conformation with respect to energy.<sup>14</sup>

Figure 2 shows the columnar structure of **1**, which runs along the *a*-axis. The molecular C<sub>3</sub> axis of the cation [Co(en)<sub>3</sub>]<sup>3+</sup> is roughly coincident with the *a*-direction. The columns are constructed by multiple hydrogen bonds between the alternately stacked cations [Co(en)<sub>3</sub>]<sup>3+</sup> and anions P<sub>3</sub>O<sub>9</sub><sup>3-</sup>.

(12) (a) Cullen, D. L.; Lingafelter, E. C. *Inorg. Chem.* **1970**, *9*, 1858. (b) Nakatsu, K.; Shiro, M.; Saito, Y.; Kuroya, H. *Bull. Chem. Soc. Jpn.* **1957**, *30*, 158.

**Figure 2.** Homochiral columnar structure of rac-[Co(en)<sub>3</sub>]P<sub>3</sub>O<sub>9</sub>·2H<sub>2</sub>O (1) running along the *a*-axis, which was constructed by the multiple hydrogen bonds between the alternately stacked cations [Co(en)<sub>3</sub>]<sup>3+</sup> and anions P<sub>3</sub>O<sub>9</sub><sup>3-</sup> with distances of N1–O5 = 2.936(6), N3–O5 = 2.896(6), N5–O7 = 2.800(5), N2–O8 = 2.900(6), N4–O8 = 2.902(5), and N6–O6 = 2.861(5) Å.

Within each column, three amine nitrogen atoms at the upper sites of one cation [Co(en)<sub>3</sub>]<sup>3+</sup> are hydrogen bonded to the oxygen atoms of one anion P<sub>3</sub>O<sub>9</sub><sup>3-</sup> with the distances of N1–O5 = 2.936(6), N3–O5 = 2.896(6), and N5–O7 = 2.800(5) Å. Three amine nitrogen atoms at the lower sites are hydrogen bonded to another P<sub>3</sub>O<sub>9</sub><sup>3-</sup> anion with the distances of N2–O8 = 2.900(6), N4–O8 = 2.902(5), and N6–O6 = 2.861(5) Å. The boat configuration of P<sub>3</sub>O<sub>9</sub><sup>3-</sup> can be produced by multiple hydrogen bonds within a column. One of the two water molecules, O11, is hydrogen-bonded to two amine nitrogens (N2 and N3) like a chelate within a column with the distances of N2–O11 = 2.981(6) and N3–O11 = 2.854(6) Å. The most striking feature is that the column is homochiral, consisting of only one of the two enantiomers,  $\Delta$ -[Co(en)<sub>3</sub>]<sup>3+</sup> and  $\Lambda$ -[Co(en)<sub>3</sub>]<sup>3+</sup>.

As shown in Figure 3b,c, four columns (two columns with the  $\Delta$  enantiomer and two columns with the  $\Lambda$  enantiomers) are connected by intercolumn hydrogen bonds to give a columnar structure along the *a*-axis, in which the anion, P<sub>3</sub>O<sub>9</sub><sup>3-</sup>, functions as a bridging group. Figure 3a shows a cross section of a cylinder. One oxygen atom of one P<sub>3</sub>O<sub>9</sub><sup>3-</sup>, O9, is hydrogen-bonded to two amine nitrogens (N1 and N6), like a chelate with distances N1–O9 = 2.926(5) and N6–

(13) (a) Pauling, L.; Sherman, J. Z. *Kristallogr.* **1937**, *96*, 481. (b) Durif, A. *Crystal Chemistry of Condensed Phosphate*; Plenum Press: New York, 1995; Chapter 4. (c) Day, V. W.; Klemperer, W. G.; Main, D. J. *Inorg. Chem.* **1993**, *32*, 1629. (d) Day, V. W.; Eberspacher, T. A.; Klemperer, W. G.; Zhong, B. J. *Am. Chem. Soc.* **1994**, *116*, 3119. (e) Day, V. W.; Klemperer, W. G. Main, D. J. *Inorg. Chem.* **1990**, *29*, 2345. (f) Averbuch-Pouchot, M. T.; Durif, A.; Guitel, J. C. *Acta Crystallogr., Sec C: Cryst. Struct. Commun.* **1988**, *C44*, 1907. (14) Day, V. W.; Klemperer, W. G.; Lockledge, S. P. Main, D. J. *J. Am. Chem. Soc.* **1990**, *112*, 2031.

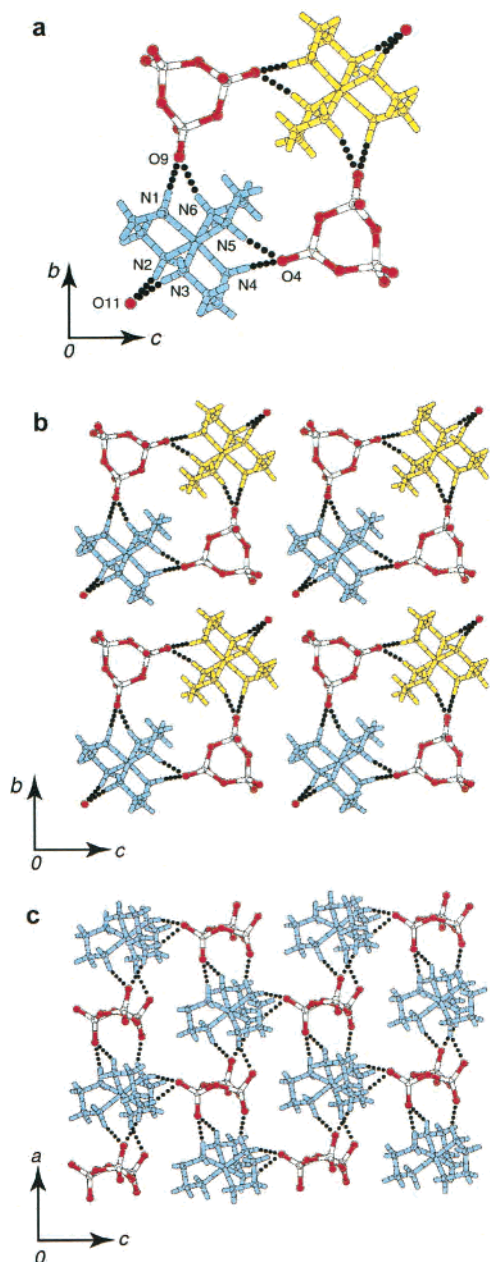


**Figure 3.** (a) Cyclic tetrameric structure of **1**, in which a  $\Delta$  enantiomer and a  $\Lambda$  enantiomer are connected by a  $\text{P}_3\text{O}_9^{3-}$  anion. (b) Crystal structure viewed down along the  $a$ -axis, showing how the cylinders are arranged along the  $a$ -axis. (c) Side view of the crystal structure, showing the intercylinder hydrogen bonds.

$\text{O9} = 2.903(5)$  Å. Another oxygen atom of the  $\text{P}_3\text{O}_9^{3-}$  anion,  $\text{O4}$ , is hydrogen-bonded to two amine nitrogens ( $\text{N4}$  and  $\text{N5}$ ), like a chelate with distances  $\text{N4}-\text{O4} = 2.999(5)$  and  $\text{N5}-\text{O4} = 2.906(6)$  Å. As a result, a cyclic tetramer is constructed. Furthermore, the tetrameric column is connected by hydrogen bonds through the water molecules. As the specific structural feature of this crystal, it should be noted that all 6 amine groups per  $[\text{Co}(\text{en})_3]^{3+}$  participate in the formation of 12 hydrogen bonds, in which 8 hydrogen bonds contribute to the construction of a homochiral column structure and the remaining 4 hydrogen bonds contribute to the tetrameric structure.

An ORTEP diagram of the unique unit of  $\Lambda$ - $[\text{Co}(\text{en})_3]\text{P}_3\text{O}_9 \cdot 2\text{H}_2\text{O}$  (**2**) with the atom numbering schemes is shown

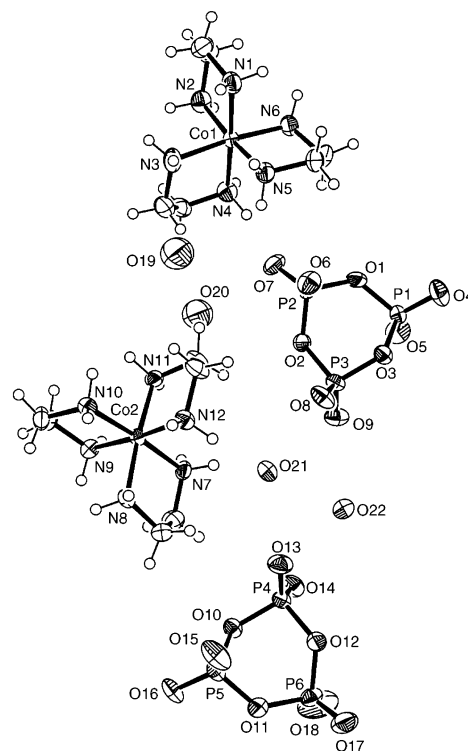


**Figure 4.** ORTEP drawing of  $\Lambda$ - $[\text{Co}(\text{en})_3]\text{P}_3\text{O}_9 \cdot 2\text{H}_2\text{O}$  (**2**) with 50% thermal probability ellipsoids and the selected atom labeling scheme.

in Figure 4. The unique unit of this crystal structure consists of two formula units ( $\Lambda$ - $[\text{Co}(\text{en})_3]\text{P}_3\text{O}_9 \cdot 2\text{H}_2\text{O}$ ). Each  $\text{Co}^{\text{III}}$  ion has a similar octahedral coordination geometry to **1** with the  $\text{N}_6$  donor atoms and the  $\text{Co}-\text{N}$  distances in the range reported for the  $\text{Co}^{\text{III}}$  complexes involving ethylenediamine. The Flack parameter refined nearly to zero ( $0.05(2)$ ), demonstrating that the two cationic complexes  $[\text{Co}(\text{en})_3]^{3+}$  in the unique unit both have the  $\Lambda$  configuration. This confirms that we synthesized the  $\Lambda$  enantiomer of  $[\text{Co}(\text{en})_3]^{3+}$  using the stereospecific synthesis described in the reference. Compound **2** assumes a homochiral column structure running along the  $a$ -axis, as shown in Figure 5 and the same as the case of **1**, which was constructed by the multiple hydrogen bonds between the cation  $[\text{Co}(\text{en})_3]^{3+}$  and anion  $\text{P}_3\text{O}_9^{3-}$  alternately stacked and the anion  $\text{P}_3\text{O}_9^{3-}$  assuming a boat configuration.

Figure 6 shows the stacking manner of the columns of **2**, in which four homochiral columns with the same chirality are connected by the intercolumn hydrogen bonds to form a cyclic tetrameric cylindrical structure and the resulting tetrameric cylinders are further combined by the hydrogen bonds. A comparison of the hydrogen bond distances of **2** with those of **1** in Table 3 may give the answer to the question “why is the heterochiral intercolumn stacking within the tetrameric cylinder preferable?” There are no intra- and intercolumn hydrogen-bond distances longer than 3.0 Å between the amine and anion or water in **1**, while there are several hydrogen bonds longer than 3.0 Å in **2**, suggesting that heterochiral intercolumn stacking is preferable.

**Circular Dichroism Spectra.** The ethylenediamine chelate ring is conformationally labile, and it takes either the  $\delta$ - or the  $\lambda$ -form. In a tris-chelate complex of ethylenedi-

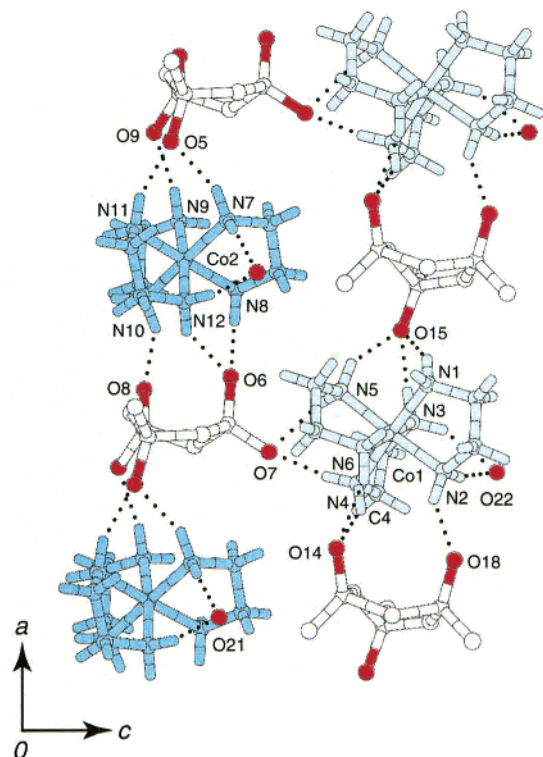


**Figure 5.** Two homochiral columns of  $\Lambda$ -[Co(en)<sub>3</sub>]P<sub>3</sub>O<sub>9</sub>·2H<sub>2</sub>O (**2**) viewed along the *a*-axis, which were constructed by multiple hydrogen bonds between alternately stacked cations [Co(en)<sub>3</sub>]<sup>3+</sup> and anions P<sub>3</sub>O<sub>9</sub><sup>3-</sup>. The two crystallographically independent units are connected by the intercolumn hydrogen bonds.

amine, [M(en)<sub>3</sub>]<sup>*n*+</sup>, the two conformations are energetically nonequivalent due to the steric interactions between adjacent pairs of chelate rings. The most stable conformation of [M(en)<sub>3</sub>]<sup>*n*+</sup> contains chelate rings in which the C–C ring bonds are nearly parallel to the C<sub>3</sub> rotation axis of the complex (the *lel*<sub>3</sub> form). For  $\Lambda$ -[M(en)<sub>3</sub>]<sup>*n*+</sup>, the order of decreasing stability follows the sequence  $\delta\delta\delta$  (*lel*<sub>3</sub>) >  $\delta\delta\lambda$  (*lel*<sub>2ob</sub>) >  $\delta\lambda\lambda$  (*lelob*<sub>2</sub>)  $\approx$   $\lambda\lambda\lambda$  (*ob*<sub>3</sub>), with an enthalpy increment of approximately 1.6 ± 0.9 kJ mol<sup>-1</sup> for each  $\delta$ (*lel*) to  $\lambda$ (*ob*) ring inversion.<sup>15</sup> In most of the  $\Lambda$ -[Co(en)<sub>3</sub>]<sup>3+</sup> crystals already analyzed, the complex ion has the *lel*<sub>3</sub> ( $\Lambda(\delta\delta\delta)$ ) conformation. The NMR spectra of the [M(en)<sub>3</sub>]<sup>*n*+</sup> complex ions indicate, however, that the most abundant conformation in solution is the intermediate *lel*<sub>2ob</sub> form and not the *lel*<sub>3</sub> form due to the entropy contribution.<sup>16</sup>

Figure 7a shows the CD spectral changes of  $\Lambda$ -[Co(en)<sub>3</sub>]-Br<sub>3</sub>·H<sub>2</sub>O as a function of the P<sub>3</sub>O<sub>9</sub><sup>3-</sup> concentration. In the absence of P<sub>3</sub>O<sub>9</sub><sup>3-</sup>, the complex exhibits a positive and a negative band at 490 and 435 nm, respectively, in the region of the octahedral d–d transition, <sup>1</sup>A<sub>1g</sub> → <sup>1</sup>T<sub>1g</sub>.<sup>17</sup> With an increase in the P<sub>3</sub>O<sub>9</sub><sup>3-</sup> concentration, the strength of the negative CD band increases at the expense of the positive CD band. Similar CD spectral changes have been reported when an oxoanion such as PO<sub>4</sub><sup>3-</sup> and SO<sub>4</sub><sup>2-</sup> is added to an

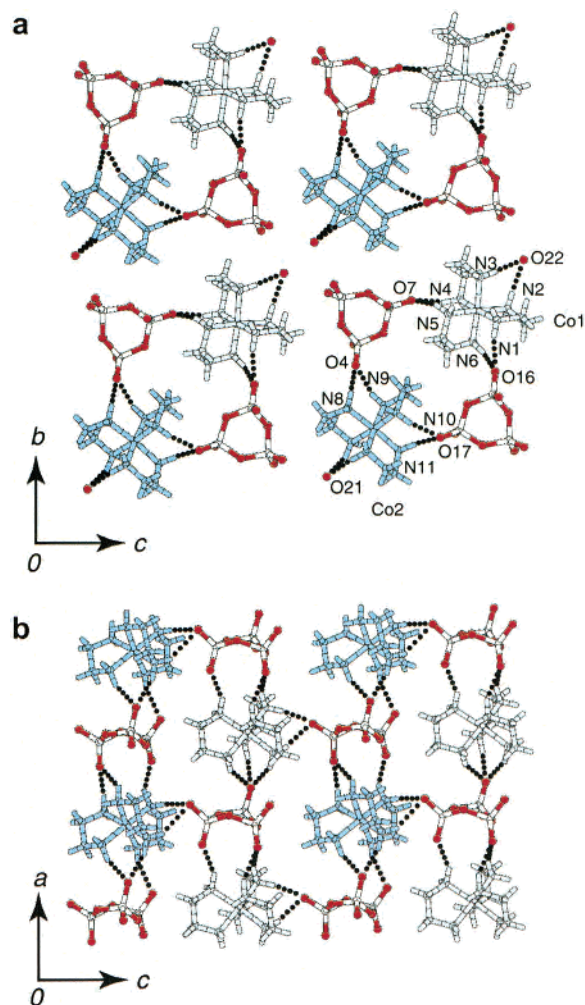


**Figure 6.** Crystal structure of **2**, in which homochiral columns with the  $\Lambda$  enantiomer are connected by the intercolumn hydrogen bonds through P<sub>3</sub>O<sub>9</sub><sup>3-</sup> anions to form a tetrameric cylindrical structure: (a) top view; (b) side view.

aqueous solution of  $\Lambda$ -[Co(en)<sub>3</sub>]<sup>3+</sup>.<sup>18</sup> Their changes have been attributed to the stabilization of the *lel*<sub>3</sub> form through ion-pair formation; an oxoanion approaches the complex cation along the C<sub>3</sub> axis such that the symmetry axes for both ions are coincident forming triple O···HN hydrogen-bonding. The generation of new chiral centers at the primary amine donors also contributes to the CD spectral changes.<sup>19</sup> The CD spectrum of  $\Lambda$ -[Co(en)<sub>3</sub>]P<sub>3</sub>O<sub>9</sub>·2H<sub>2</sub>O in a KBr disk exhibits a relatively strong negative CD band at 445 nm in accordance with the *lel*<sub>3</sub> conformation in the crystal (Figure 7b).

**Conductivity Measurements.** The cation–anion association behavior between *rac*-[Co(en)<sub>3</sub>]<sup>3+</sup> and P<sub>3</sub>O<sub>9</sub><sup>3-</sup> in aqueous solution has been studied by quantitative analysis of the conductivity measurements.<sup>20</sup> Figure 8 shows the plots of equivalent conductivity  $\Lambda^0$  vs the square root of the equivalent concentration  $C^{*1/2}$  for Na<sub>3</sub>P<sub>3</sub>O<sub>9</sub>·H<sub>2</sub>O and *rac*-[Co(en)<sub>3</sub>]Cl<sub>3</sub>·3H<sub>2</sub>O, together with their least-squares lines. Each plot obeys the equation of  $\Lambda = \Lambda^0 - AC^{*1/2}$ , demon-

(15) (a) Corey, E. J.; Bailar, J. C., Jr. *J. Am. Chem. Soc.* **1959**, *81*, 2620. (b) Niketic, S. R.; Rasmussen, K. *Acta Chem. Scand.* **1978**, *A32*, 391.  
 (16) Sudmeier, J. L.; Blackmer, G. L.; Bradley, C. H.; Anet, F. A. L. **1972**, *94*, 757.  
 (17) (a) McCaffery, A. J.; Mason, S. F. *Mol. Phys.* **1963**, *6*, 359. (b) Mason, S. F.; Peart, B. J. *J. Chem. Soc., Dalton Trans.* **1977**, 935.

(18) (a) Mason, S. F.; Norman, B. J. *Proc. Chem. Soc.* **1964**, 339. (b) Mason, S. F.; Norman, B. J. *J. Chem. Soc. A* **1966**, 307.  
 (19) Sarneski, J. E.; Urbach, F. L. *J. Am. Chem. Soc.* **1971**, *93*, 884.  
 (20) Onsager, L. *Z. Phys.* **1927**, *28*, 277.

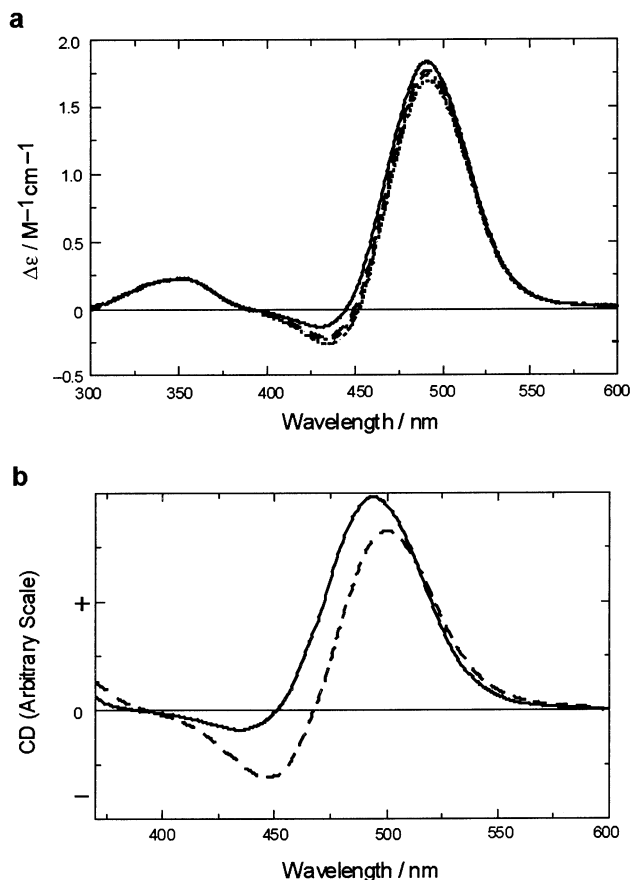


**Figure 7.** (a) CD spectra of  $\Lambda$ -[Co(en)<sub>3</sub>]Br<sub>3</sub>·H<sub>2</sub>O ( $2.50 \times 10^{-3}$  M) as a function of Na<sub>3</sub>P<sub>3</sub>O<sub>9</sub>·H<sub>2</sub>O concentration ( $0$ – $2.5 \times 10^{-2}$  M). With an increase in the P<sub>3</sub>O<sub>9</sub><sup>3-</sup> concentration, the strength of the negative CD band around 435 nm increases at the expense of that of the positive CD band around 490 nm. (b) CD spectra of  $\Lambda$ -[Co(en)<sub>3</sub>]Br<sub>3</sub>·H<sub>2</sub>O (—) and  $\Lambda$ -[Co(en)<sub>3</sub>]P<sub>3</sub>O<sub>9</sub>·2H<sub>2</sub>O (---) in KBr disks.

strating that there is no cation–anion association both in Na<sub>3</sub>P<sub>3</sub>O<sub>9</sub>·H<sub>2</sub>O and *rac*-[Co(en)<sub>3</sub>]Cl<sub>3</sub>·3H<sub>2</sub>O. The equivalent ionic conductivities,  $\Lambda^0$ , of [Co(en)<sub>3</sub>]Cl<sub>3</sub>·3H<sub>2</sub>O and Na<sub>3</sub>P<sub>3</sub>O<sub>9</sub>·H<sub>2</sub>O in aqueous solution at 25 °C at infinite dilution have been determined to be 153.8 and 132.2, respectively, according to Onsager's method.<sup>20</sup> On the basis of  $\Lambda^0 = \Lambda^0(+)+\Lambda^0(-)$ , the equivalent ionic conductivity of *rac*-[Co(en)<sub>3</sub>]<sup>3+</sup> at infinite dilution was found to be  $\Lambda^0(+)=77.4$  by subtracting the reported value of  $\Lambda^0(-)$  for Cl<sup>-</sup>.<sup>21</sup> Similarly the equivalent ionic conductivity of P<sub>3</sub>O<sub>9</sub><sup>3-</sup> at infinite dilution was found to be  $\Lambda^0(-)=82.1$ , whose value well agrees with the value reported by Davies and Monk.<sup>22</sup>

If there was no cation–anion association between *rac*-[Co(en)<sub>3</sub>]<sup>3+</sup> and P<sub>3</sub>O<sub>9</sub><sup>3-</sup>, the equivalent conductivity of *rac*-[Co(en)<sub>3</sub>](P<sub>3</sub>O<sub>9</sub>)·2H<sub>2</sub>O should follow the equation of  $\Lambda = \Lambda^0 - AC^{*1/2}$  with  $\Lambda^0 = 77.4 + 82.1 = 159.5$  and  $A = 1166$ , where the former value was experimentally obtained as described above and the latter value was theoretically evaluated according to the references. Figure 8 also shows the theoretical line with the parameters and the experimental plots of  $\Lambda$  vs  $C^{*1/2}$  for *rac*-[Co(en)<sub>3</sub>](P<sub>3</sub>O<sub>9</sub>)·2H<sub>2</sub>O. The

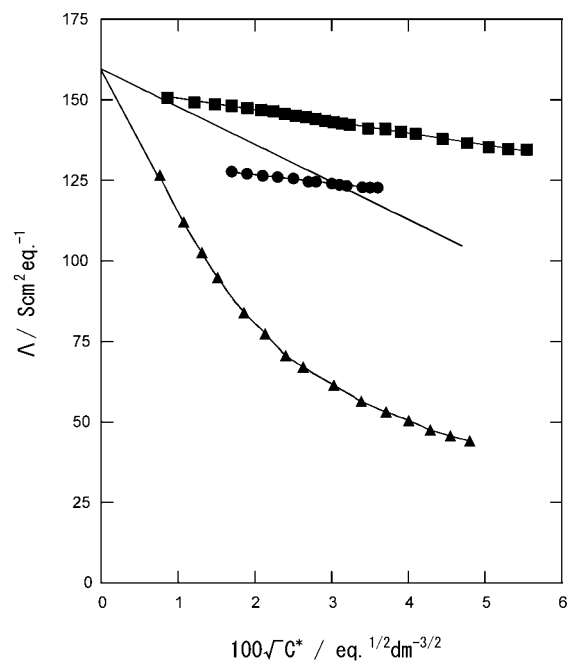


**Figure 8.** Plots of equivalent conductance  $\Lambda$  vs square root of equivalent concentrations,  $C^{*1/2}$ , for *rac*-[Co(en)<sub>3</sub>]Cl<sub>3</sub>·2H<sub>2</sub>O (■), Na<sub>3</sub>P<sub>3</sub>O<sub>9</sub>·H<sub>2</sub>O (●), and *rac*-[Co(en)<sub>3</sub>]P<sub>3</sub>O<sub>9</sub>·2H<sub>2</sub>O (▲) in aqueous solutions at 25 °C. The solid lines follow the theoretical lines of equation of  $\Lambda = \Lambda^0 - AC^{*1/2}$  with the parameters of  $\Lambda^0 = 153.8$  and  $A = 224$  for *rac*-[Co(en)<sub>3</sub>]Cl<sub>3</sub>·2H<sub>2</sub>O and with  $\Lambda^0 = 132.2$  and  $A = 317$  for Na<sub>3</sub>P<sub>3</sub>O<sub>9</sub>·H<sub>2</sub>O, respectively. The solid line for *rac*-[Co(en)<sub>3</sub>]P<sub>3</sub>O<sub>9</sub>·2H<sub>2</sub>O is the theoretical line of  $\Lambda = \Lambda^0 - AC^{*1/2}$  with  $\Lambda^0 = 159.5$  and  $A = 1166$ .

theoretical line of *rac*-[Co(en)<sub>3</sub>](P<sub>3</sub>O<sub>9</sub>)·2H<sub>2</sub>O is steeper than those of Na<sub>3</sub>P<sub>3</sub>O<sub>9</sub>·H<sub>2</sub>O and *rac*-[Co(en)<sub>3</sub>]Cl<sub>3</sub>·3H<sub>2</sub>O, and the steepness is ascribed to the 3+ : 3- ionic atmosphere of *rac*-[Co(en)<sub>3</sub>]<sup>3+</sup> and P<sub>3</sub>O<sub>9</sub><sup>3-</sup>. The experimental plots of *rac*-[Co(en)<sub>3</sub>](P<sub>3</sub>O<sub>9</sub>)·2H<sub>2</sub>O deviate far below the theoretical line, and the equivalent conductivity abruptly decreases with the increase in  $C^{*1/2}$ , indicating a strong cation–anion association.

The Debye–Huckel theory<sup>23</sup> can be applied under dilute concentrations below 0.01 M, in which the plots of the  $\log K$  vs  $I^{1/2}$  are linear and the thermodynamic association constant,  $\log K^0$ , can be obtained by extrapolation of the ionic strength to zero. From the conductivity data, plots of  $\Lambda$  vs  $C^{*1/2}$ , the degree of dissociation  $\alpha$ , and the thermodynamic association constant  $K$  of the ion-pair *rac*-[Co(en)<sub>3</sub>]<sup>3+</sup>–P<sub>3</sub>O<sub>9</sub><sup>3-</sup> at each concentration can be determined, where  $\alpha = \Lambda/\Lambda^0$ ,  $K = \frac{[\text{Co(en)}_3\text{P}_3\text{O}_9]}{[\text{Co(en)}_3]^{3+}[\text{P}_3\text{O}_9]^{3-}} = \frac{C(1-\alpha)}{C\alpha^2}$ , and  $C$  is the total concentration. The ionic strength,  $I$ , can be derived from the equation of  $I = 9C\alpha$ . Plots of  $\log K$  vs  $I^{1/2}$  are shown in Figure 9. The linearity indicates that the Debye–Huckel theory can be applied. The thermodynamic association constant,  $\log K^0 = 4.26$ , and the Gibbs free energy,  $\Delta G = -24.3$  k J mol<sup>-1</sup>, were obtained. The thermodynamic association constant obtained from these plots is greater than  $\log K^0 = 3.58$  of [Co(NH<sub>3</sub>)<sub>6</sub>]<sup>3+</sup> and SO<sub>4</sub><sup>2-</sup> reported by Katayama et al.<sup>24</sup> A comparison of the thermodynamic association constant with the theoretical value can provide insight into the cation–anion interaction. A theoretic-

(21) Robinson, R. A.; Stokes, R. H. *Electrolyte Solutions*; Butterworths: London, 1959.

(22) Davies, C. W.; Monk, C. B. *J. Chem. Soc.* **1949**, 413.

(23) Debye, P.; Huckel, E. *Phys. Z.* **1923**, *24*, 185.

(24) Katayama, S.; Tamamushi, R. *Bull. Chem. Soc. Jpn.* **1970**, *43*, 2354.

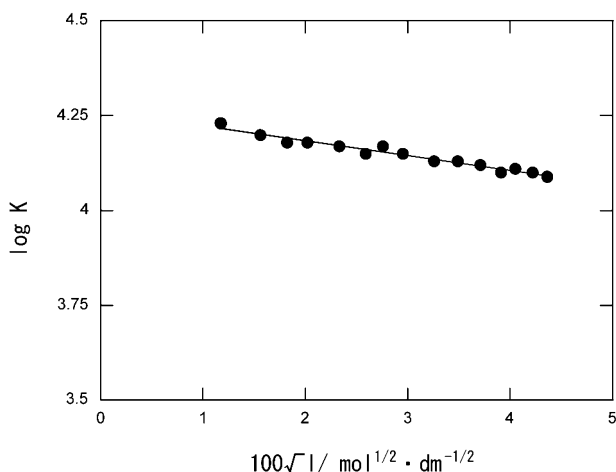


**Figure 9.** Plots of  $\log K$  vs  $100I^{1/2}$  for *rac*-[Co(en)<sub>3</sub>]P<sub>3</sub>O<sub>9</sub>·2H<sub>2</sub>O in aqueous solution at 25 °C.

cal electrostatic cation–anion association constant,  $K_f$ , in aqueous solution, can be calculated using the Fuoss equation.<sup>25</sup> Values of  $K_f = 1550 \text{ mol}^{-1} \text{ dm}^3$  and  $\Delta G_f = -18.2 \text{ kJ mol}^{-1}$  were calculated from the equation  $\Delta G_f = -RT \ln K_f$ . The Gibbs free energy of  $\Delta G = -24.3 \text{ kJ mol}^{-1}$  is substantially lower than the theoretical value, and the difference,  $\Delta = -6.1 \text{ kJ mol}^{-1}$ , can be ascribed mainly to a hydrogen bond formation and conformational changes in the P<sub>3</sub>O<sub>9</sub><sup>3-</sup> anion. Since the conformation changes from a stable chair form to an unstable boat form, P<sub>3</sub>O<sub>9</sub><sup>3-</sup> contributes to destabilization, while the stabilization energy due to the hydrogen bond formation is much larger than  $\Delta = -6.1 \text{ kJ mol}^{-1}$ . The large excess Gibbs free energy may also be consistent with the fact that the CD spectra of [Co(en)<sub>3</sub>]<sup>3+</sup> changed to the negative direction with an increase in the P<sub>3</sub>O<sub>9</sub><sup>3-</sup> concentration.

## Experimental Section

**Materials.** All chemicals and solvents used for the synthesis were reagent grade, obtained from commercial suppliers, and used without further purification. Reagents used for the physical measurements were of spectroscopic grade.

**Na<sub>3</sub>P<sub>3</sub>O<sub>9</sub>·H<sub>2</sub>O.** This compound was prepared by a modification of the method reported by Thilo and Grunze.<sup>26</sup> Sodium dihydrogen phosphate (50 g) was heated in an electric furnace at 1000 °C for 2 h. The temperature was then lowered to 520 °C, and the resulting material was heated at that temperature for 12 h. The crude product was dissolved in water and filtered. Ethanol was slowly added to the filtrate to precipitate Na<sub>3</sub>P<sub>3</sub>O<sub>9</sub>·H<sub>2</sub>O. The hydration number was determined by TGA and DTA. The observed weight loss of 5.2% corresponds to the elimination of 1 water molecule/Na<sub>3</sub>P<sub>3</sub>O<sub>9</sub>·H<sub>2</sub>O (calcd 5.6%). Mp: 611.8 °C.

**rac-[Co(en)<sub>3</sub>]P<sub>3</sub>O<sub>9</sub>·2H<sub>2</sub>O (1).** [Co(en)<sub>3</sub>]Cl<sub>3</sub>·3H<sub>2</sub>O<sup>27</sup> (0.80 g, 2.0 mmol) in 5 mL of water was added to a solution of Na<sub>3</sub>P<sub>3</sub>O<sub>9</sub>·H<sub>2</sub>O (0.82 g, 2.5 mmol) in 7 mL of water, and the mixture was evaporated slowly at room temperature. Orange crystals, which had formed, were collected by filtration and dried in air. Yield: 0.33 g. Anal. Calcd for C<sub>6</sub>H<sub>28</sub>N<sub>6</sub>CoO<sub>11</sub>P<sub>3</sub> = [Co(en)<sub>3</sub>]P<sub>3</sub>O<sub>9</sub>·2H<sub>2</sub>O: C, 14.07; H, 5.51; N, 16.41. Found: C, 14.25; H, 5.48; N, 16.54.

(25) Fuoss, R. *J. Am. Chem. Soc.* **1958**, *80*, 5059.

(26) Thilo, E.; Grunze, H. *Z. Anorg. Allg. Chem.* **1955**, *281*, 263.

(27) Work, J. B. *Inorg. Synth.* **1946**, *2*, 221.

**$\Lambda$ -[Co(en)<sub>3</sub>]P<sub>3</sub>O<sub>9</sub>·2H<sub>2</sub>O (2).**  $\Lambda$ -[Co(en)<sub>3</sub>]Cl<sub>3</sub>·H<sub>2</sub>O<sup>29</sup> (0.36 g, 1.0 mmol) in water (5 mL) was added to a suspension of Ag<sub>3</sub>P<sub>3</sub>O<sub>9</sub>·H<sub>2</sub>O<sup>28</sup> (0.58 g, 1.0 mmol) in water (20 mL). After about 1 h of mechanical stirring, AgCl was filtered off, and the filtrate was slowly evaporated at room temperature to yield orange plates. These were collected by filtration and recrystallized from water (7 mL). Yield: 0.13 g. Anal. Calcd for C<sub>6</sub>H<sub>28</sub>N<sub>6</sub>CoO<sub>11</sub>P<sub>3</sub> = [Co(en)<sub>3</sub>]P<sub>3</sub>O<sub>9</sub>·2H<sub>2</sub>O: C, 14.07; H, 5.51; N, 16.41. Found: C, 14.18; H, 5.46; N, 16.31.

**Physical Measurements.** Elemental analyses for C, H, and N were performed at the Elemental Analyses Service Center of Kyushu University. Thermogravimetric and differential thermal analyses (TGA and DTA) were carried out on a Seiko Instruments, Type TA SSC5000, in an air flow at a heating rate of 10 °C/min. Al<sub>2</sub>O<sub>3</sub> was used as the reference sample. Circular dichroism (CD) spectra were measured with a JASCO J-720 spectropolarimeter. An aliquot of Na<sub>3</sub>P<sub>3</sub>O<sub>9</sub>·H<sub>2</sub>O was added to a 5 mM aqueous solution of  $\Lambda$ -[Co(en)<sub>3</sub>]Br<sub>3</sub>·H<sub>2</sub>O, and the CD spectral changes were measured in the range 300–600 nm. The conductivity measurements were performed with a TOA Co., Ltd., conductometer, model CM-5S, and a cell (Type CG-511B, cell constant 0.964). The temperature of the sample was precisely controlled at 25.0 ± 0.1 °C in a thermostat bath. The pH of the solution was maintained between 6.5 and 7.0.

**X-ray Data Collection, Reduction, and Structure Determination.** X-ray data were collected on a Rigaku RAXIS–RAPID image plate diffractometer with graphite-monochromated Mo K $\alpha$  radiation ( $\lambda = 0.71069 \text{ \AA}$ ). The data were collected at a temperature of 25 °C to a maximum  $2\theta$  value of 55.0°. A numerical absorption correction using the program NUMABS was applied.<sup>30</sup> The data were also corrected for Lorentz and polarization effects.

The structures were solved by heavy-atom Patterson methods<sup>31</sup> and expanded using the Fourier technique.<sup>31</sup> The non-hydrogen atoms were refined anisotropically. Hydrogen atoms, at their calculated positions, were included in the structure factor calculations but not refined. Full-matrix least-squares refinement based on the observed reflections was employed. The unweighted and weighted agreement factors of  $R = \sum |F_o| - |F_c| / \sum |F_o|$  for  $I > 2.0\sigma(I)$  and  $R_w = [\sum w(|F_o|^2 - |F_c|^2)^2 / \sum w|F_o|^2]^2$  for all data were used, respectively. Neutral atomic scattering factors were taken from Cromer and Waber.<sup>32</sup> Anomalous dispersion effects were included in  $F_c$ ; the values  $\Delta f'$  and  $\Delta f''$  were those of Creagh and McAuley.<sup>33</sup> The values for the mass attenuation coefficients were those of Creagh and Hubbel.<sup>34</sup> All calculations were performed using the teXsan crystallographic software package.<sup>35</sup>

(28) Durif, A. *Crystal Chemistry of Condensed Phosphates*; Plenum: New York, 1995.

(29) Broomhead, J. A.; Dwyer, F. P.; Hogarth, J. W. *Inorg. Synth.* **1960**, *6*, 183.

(30) Higashi, T. *NUMABS: Program for Absorption Correction*; Rigaku Corp.: Tokyo, 1999.

(31) PATTY and DIRDIF94: Beurskens, P. T.; Admiraal, G.; Beurskens, G.; Bosman, W. P.; de Gelder, R.; Israel, R.; Smits, J. M. M. *The DIRDIF-94 program system*; Technical Report of the Crystallography Laboratory; University of Nijmegen: Nijmegen, The Netherlands, 1999.

(32) Cromer, D. T.; Waber, J. T. *International Tables for X-ray Crystallography*; The Kynoch Press: Birmingham, England, 1974; Vol. IV, Table 2.2 A.

(33) Creagh, D. C.; McAuley, W. J. *International Tables for Crystallography*; Wilson, A. J. C., Ed.; Kluwer Academic Publishers: Boston, MA, 1992; Vol. C, Table 4.2.6.8, pp 219–222.

(34) Creagh, D. C.; Hubbell, J. H. *International Tables for Crystallography*; Wilson, A. J. C., Ed.; Kluwer Academic Publishers: Boston, MA, 1992; Vol. C, Table 4.2.4.3, pp 200–206.

(35) *teXsan: Crystal Structure Analysis Package*; Molecular Structure Corp.: The Woodlands, TX, 1985, 1999.

**Acknowledgment.** The authors acknowledge Prof. Y. Ishii, Department of Chemistry and Biotechnology, Graduate School of Engineering, The University of Tokyo, for his valuable discussions.

**Supporting Information Available:** X-ray crystallographic files in CIF format for compounds **1** and **2**. This material is available free of charge via the Internet at <http://pubs.acs.org>.

IC0260623